Classical topological paramagnetism

R. Bondesan and Z. Ringel
Theoretical Physics, Oxford University, 1, Keble Road, Oxford OX1 3NP, United Kingdom
(Received 18 July 2016; revised manuscript received 4 April 2017; published 11 May 2017)

Topological phases of matter are one of the hallmarks of quantum condensed matter physics. One of their striking features is a bulk-boundary correspondence wherein the topological nature of the bulk manifests itself on boundaries via exotic massless phases. In classical wave phenomena, analogous effects may arise; however, these cannot be viewed as equilibrium phases of matter. Here, we identify a set of rules under which robust equilibrium classical topological phenomena exist. We write simple and analytically tractable classical lattice models of spins and rotors in two and three dimensions which, at suitable parameter ranges, are paramagnetic in the bulk but nonetheless exhibit some unusual long-range or critical order on their boundaries. We point out the role of simplicial cohomology as a means of classifying, writing, and analyzing such models. This opens an experimental route for studying strongly interacting topological phases of spins.

DOI: 10.1103/PhysRevB.95.174418

I. INTRODUCTION

Symmetry-protected topological (SPT) phases are exotic quantum states of matter that are featureless in the bulk but still support unusual low-energy phenomena on their boundaries. Their distinguishing properties remain sharp and robust as long as the appropriate symmetries are maintained. An important example is the quantum spin Hall insulator [1], protected by time-reversal symmetry, whose edge physics may be used in spintronics [2–4] and in the creation of topologically protected qubits in the form of Majorana fermions [5]. Partially motivated by the search for other exotic boundary phenomena, the field has developed rapidly: The classification table of weakly interacting topological phases of electrons given various symmetries has been established [6] in what can be seen as a modern revival of band structure theory. Furthermore, various topological electronic phases have been realized [1,7]. Turning to bosons, a difficulty arises since without interactions their ground state is always a superfluid regardless of the band structure. Nonetheless, such phases do exist at strong interactions and are known as bosonic SPTs [8–10]. Unfortunately, experimental realizations of bosonic SPTs are scarce and, to the best of our knowledge, limited to one-dimensional (1D) spin chains [11].

Recently, there has been both theoretical [12–14] and experimental [15–20] interest in the notion of classical topological phases mimicking the phenomenology of their quantum counterparts. A typical strategy there is to consider systems of springs and masses or optical devices which have an underlying topological band structure. Their edges can be seen as robust waveguides which have potential engineering applications, such as delay lines for light and sound [21]. Notwithstanding, it is difficult to view such phenomena as a distinct phase of matter since the topological nature of the band structure does not induce any sharp measurable features in equilibrium. Further, at present the effect of nonlinearities on these systems is unclear. (See, however, [20].) Both these issues can be seen as a classical reflection of the aforementioned difficulty of finding topological equilibrium phases of noninteracting bosons. As in the quantum case, an alternative route may thus be to consider strongly interacting systems.

One approach to obtain such models is to start from known quantum SPT models and attempt to write their discretized Euclidean time partition function in a sign-problem-free and local manner. When possible, the resulting partition function can then be viewed as a classical statistical mechanical system. Nonetheless, the models thus obtained have several drawbacks. First, the notion of symmetry protection does not generally carry through to the classical problem, in the following sense: We define classical symmetries as those one-to-one maps on configuration space which leave the Boltzmann weight invariant. For instance, in a spin-1 antiferromagnetic chain which supports a 1D SPT known as the Haldane phase [22], the associated classical configuration space is one discrete variable ($m_z = -1,0,1$) per site. When viewed as an SPT phase protected by SO(3) or its $Z_2 \times Z_2$ subgroup of π rotations [23], the action of the symmetry involves superpositions and cannot be considered classical. A related issue is that the microscopic mechanism stabilizing topological phases, based on matrix product states and projective symmetries [10], becomes obfuscated in the classical setting. Lastly, the Boltzmann weights resulting from the prescription outlined above, are complicated and anisotropic, making these models less experimentally relevant.

Interestingly, for some models based on coupled superfluids, the lattice Euclidean time partition function, following a series of transformations, can be written in a sign-free manner [24]. The advantage here is that the resulting models are isotropic. However, in the process of making the action local, additional degrees of freedom are introduced and, from a classical perspective, it is thus unclear what are the essential ingredients which render this a well-defined classical phase of matter rather than a particular model. Furthermore, it will be useful to generalize this approach to the discrete symmetry case which is more experimentally relevant.

In this work, we address the question of what restrictions, analogous to symmetry protection, should be imposed on a classical system under which it supports robust classical topological phases (CTPs). The first requirement is to consider systems invariant under a group G and a local constraint whose defects carry elements of another group G'. (More details about defects can be found in the Appendix.) One example would be a gauge theory with gauge group G' and defects being

monopoles. The second requirement is that these phases must be short-range correlated in the bulk and in particular must not break the symmetry spontaneously. The third is that they must confine defects of the constraints into neutral pairs (see the Appendix for a precise definition). We refer to phases which obey the above restrictions as "admissible phases."

Interestingly, we find that given a dimension d, and the groups G, and G' as above, there are many inequivalent admissible phases. As standard, two phases are deemed equivalent if a continuous deformation from one to another is possible without crossing a critical point. By continuous we mean that one deforms the energy functional gradually and maintains the local constraint. We establish the existence of inequivalent phases by providing concrete examples of models between which any continuous deformation must involve a phase transition. Notably, given that such distinct phases exist, by definition their distinction does not involve a local order parameter or confinement-deconfinement transitions. Their difference is of topological origin. This is manifested on interfaces between distinct phases, where either long-range correlated or quasi-long-range correlated phases emerge.

In the next sections, we will explore these ideas for the choice $G = G' = Z_N$, considering models in both two and three dimensions [(2D) and (3D)] where we find many distinct topological phases with the accompanying exotic boundary phenomena. The latter include a "forbidden" [25] symmetry-breaking order along 1D boundary and an unusual 2D critical phase corresponding to a theory of a compact boson in which the basic $\pm 2\pi$ vortices are linearly confined. Just as group cohomology was shown to be the basis for quantum SPT phases, we will show that tools from cellular cohomology [26] give a powerful mathematical framework for writing models of CTPs and analyzing them. The models thus produced are compact, isotropic, and, to a large extent, analytically tractable, thereby increasing both their theoretical and experimental relevance. The $G = G' = \mathbb{Z}_2$ models in 2D and 3D are further shown to be in the same universality class as the imaginary time partition function of certain 1D and 2D models (the group cohomology models [8]) of bosonic SPTs. From a numerical perspective, our models thus provide an efficient way for performing Monte Carlo simulations of bosonic SPTs with discrete symmetries (see also Ref. [24] for the continuous case). They also open a promising experimental route for studying these fascinating strongly interacting phases of matter.

II. TWO DIMENSIONS

As a first illustrative example of a 2D CTP with $G = \mathbb{Z}_2$ we consider the following model on the square lattice:

$$Z = \sum_{\sigma,U} e^{-\beta\mathscr{H}} \prod_p \delta(U_{ij}U_{jk}U_{kl}U_{li} - 1), \tag{1}$$

$$-\beta\mathscr{H} = \sum_{\langle i,j\rangle} \{K_1\sigma_i U_{ij}\sigma_j + K_2 U_{ij}\}. \tag{2}$$

Here, $\sigma_i = \pm 1$ and $U_{ij} = \pm 1$ are site and link variables, and the product is over plaquettes p, having the sites i,j,k,l on their boundary. The model has a $\mathbb{Z}_2$ symmetry $\sigma_i \to -\sigma_i$, and it has a $\mathbb{Z}_2$ constraint forcing zero flux for the U field through each plaquette.

Conveniently, a nonlocal transformation ($U_{ij} = \mu_i\mu_j$) maps this model to two decoupled Ising models, and has thus $\mathbb{Z}_2 \times \mathbb{Z}_2$ symmetry:

$$Z = \sum_{\sigma,\mu} \exp \sum_{\langle i,j\rangle} \{K_1\rho_i\rho_j + K_2\mu_i\mu_j\}, \qquad \rho_i = \sigma_i\mu_i. \tag{3}$$

Denoting $K_c = -\frac{1}{2}\ln\tanh K_c$ the critical coupling of the Ising model on a square lattice, there are two regimes which are of interest to us: the trivial phase ($K_2 > K_c > K_1 \geqslant 0$) where $\langle\mu_i\rangle \neq 0$, and the nontrivial phase ($K_1 > K_c > K_2 \geqslant 0$) where $\langle\rho_i\rangle \neq 0$. The other variables ρ and σ for the trivial case and μ and σ for the nontrivial are disordered. Notably, in both cases U_{ij}'s are uncorrelated, namely $\langle(U_{ij} - \langle U_{ij}\rangle)(U_{kl} - \langle U_{kl}\rangle)\rangle$ is exponentially decaying.[1] We remark that the partition function of Eq. (2) with constraint violations at two plaquettes equals that of Eq. (3) where the sign of both couplings K_1, K_2 is reversed along a path connecting the two plaquettes [27]. Thus, for both regimes, the presence of order parameters with long-range order implies linear confinement of the defects.

In terms of ρ and μ, the model is simply two decoupled ferromagnets that exhibit symmetry-broken phases. However, in the original degrees of freedom U,σ, the physical properties of the two phases change. Considering bulk physics, long-range order in ρ implies the following nonlocal (string) order parameter in the nontrivial phase:

$$\langle\rho_i\rho_j\rangle = \left\langle \sigma_i \prod_{\ell\in\Gamma_{ij}} U_\ell\sigma_j \right\rangle \to \text{const} \tag{4}$$

as $\text{dist}(i,j) \to \infty$ and Γ_{ij} is a path from i to j. Alternatively stated, performing the nonlocal transformation $\sigma_i \to \rho_i = \prod_{\ell\in\Gamma_{0i}} U_\ell\sigma_i$, with 0 a reference site, unveils a hidden ferromagnetic phase for the nontrivial order, whereas for the trivial phase, this results in a simple paramagnet.

As we now argue, the hidden ferromagnetic order is a distinguishing property of the topological phase and therefore one cannot continuously deform the models onto one another. This implies that there are at least two distinct admissible phases in our classification for $d = 2$, $G = G' = Z_2$. Notably, local and symmetric perturbations in the original U and σ variables would be transformed into local and symmetric perturbations in μ and σ. As this transformation has no effect on the free energy, one finds that hidden order is thermodynamically equivalent to conventional order. This means that hidden order is not just a feature of the model but rather a robust property which can only vanish through a phase transition or by leaving the space of admissible phases.

Perhaps the most interesting distinction between these two phases comes about when considering a 1D interface between them. In general, near an interface between a ferromagnet and

[1] We remark that one can consider more general couplings, such as those of the Ashkin-Teller model [33], as long as the set of order parameters in a phase is unchanged. Our choice of two decoupled Ising models is made for pedagogical purposes.

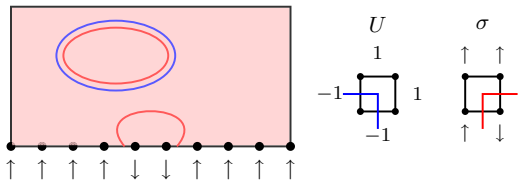

FIG. 1. Pictorial representation of low-energy configurations of the 2D classical topological paramagnet. Red lines are domain walls of the spins, while the blue ones are those where the link variable $U = -1$. In the bulk, both of these lines must form closed paths and energetically they are also encouraged to pair up, and at a boundary (bottom) σ has long-range order.

a paramagnet, the order parameter leaks into the paramagnetic phase up to some penetration length. Similarly, close to an interface between the above two phases, both order parameters (ρ and μ) will be ordered and as a result $\sigma = \rho \cdot \mu$ would also be ordered, despite being disordered in the bulk on both sides. For instance, setting $K_1 = 0$, $K_2 \to \infty$ on the trivial side is equivalent to placing the nontrivial phase in an open geometry with boundary conditions $U_{ij} = 1$ or equivalently $\mu_i = \mu_j$, implying long-range order for σ.

More physically, one can view the configurations of U in (1) as polygons on the dual lattice by assigning a line of the polygon to links across which $U = -1$. The K_1 coupling then encourages domain walls of the spins to attach to these polygons. Kinks of σ along the interface are necessarily ends of domain walls in the bulk. However, these domain walls cannot have an accompanying polygon as the latter is confined from entering the trivial phase (vacuum in the picture). Consequently, the bulk, despite being locally disordered, linearly confines kinks of σ at the boundary into neutral pairs (see Fig. 1).

A. Relation with the AKLT Hamiltonian

We now establish a precise connection between the 2D CTP presented and the Affleck-Kennedy-Lieb-Tasaki (AKLT) model, the paradigmatic example of a quantum SPT phase of spins in (1 + 1)D [22]. (See also [28] for a picture of AKLT that is close to our construction.) We consider the transfer matrix of the 2D CTP in the limit of anisotropic coupling $K_i^x = \epsilon\lambda_i$, $e^{-2K_i^y} = \epsilon\lambda_i'$, $i = 1,2$, along the horizontal (x) or vertical direction (y). It is then a standard exercise (see, e.g., [29]) to derive the quantum Hamiltonian in the limit $\epsilon \to 0$ starting from Eq. (3) in the main paper, and to pass from the μ variables to their duals τ. This results in the $\mathbb{Z}_2 \times \mathbb{Z}_2$ symmetric Hamiltonian $H = H_0 + \sum \lambda_2 \tau^x_{i+1/2} + \lambda_1' \sigma_i^x$, where

$$H_0 = \sum \lambda_1 \sigma_i^z \tau^x_{i+1/2} \sigma^z_{i+1} + \lambda_2' \tau^z_{i-1/2} \sigma_i^x \tau^z_{i+1/2}, \tag{5}$$

and which coincides with the AKLT Hamiltonian in the form considered in [30] for $\lambda_1 = \lambda_2'$. Having equivalent phenomenology and a very similar algebraic structure strongly suggests that these two models describe the same phase. Interestingly, when expressing our model in terms of the dual variables τ, the Boltzmann weights are not positive anymore. The $\mathbb{Z}_2$ constraint thus appears as a natural way to reflect the additional $\mathbb{Z}_2$ symmetry while maintaining positive Boltzmann weights and locality.

B. Generalizations to $G = G' = Z_N$

Let us generalize the above model to the case $G = G' = Z_N$. Accordingly, we consider a directed square lattice and take $\sigma_i \in \mathrm{Z}_N$ and $U_{ij} = U_{ji}^{-1} \in \mathrm{Z}_N$ for the orientation being from vertex i to j. We represent elements in Z_N by $e^{2\pi i\alpha/N}$, $\alpha = 0,1,\ldots,N-1$. For a given $p = 0,1,\ldots,N-1$, let us define the minimal coupling:

$$\mathscr{H}_p = \sum_i \sum_{j\sim i} \sigma_i^p U_{ij} \sigma_j^{-p}, \tag{6}$$

where $j \sim i$ means j a neighbor of i, so that each edge is counted twice, once with its positive and once with its negative orientation ensuring a real energy. Given nonzero $p \neq p'$ the generalized model is defined by (1) with

$$-\beta\mathscr{H}_{p,p'} = K_1\mathscr{H}_p + K_2\mathscr{H}_{p'}. \tag{7}$$

As we will show, for large K_1 (K_2), p (p') controls the topological index. Let us note that σ^p is a $\mathbb{Z}_N$ variable only when p and N are coprime. Otherwise, it has a reduced order, given by N/p. In order to keep the physical message of this section clear and concise, we do not delve here in these number theoretic considerations, and assume N to be prime.

To analyze the model we first expose the hidden order. To this end, we resolve the constraint using

$$U_{ij} = \mu_i \mu_j^{-1} \tag{8}$$

yielding

$$\mathscr{H}_p = \sum_i \sum_{j\sim i} \sigma_i^p \mu_i \mu_j^{-1} \sigma_j^{-p} \tag{9}$$

and

$$Z = \frac{1}{N} \sum_{\sigma,\mu} e^{-\beta\mathscr{H}}, \tag{10}$$

where the factor of $\frac{1}{N}$ comes from the 1 to N mapping between U_{ij} which respect the constraint and μ_i.

Next, we wish to go to the composite variables

$$\tilde{\sigma}_{i;p} = \mu_i \sigma_i^p, \quad \tilde{\mu}_{i;p'} = \mu_i \sigma_i^{p'}. \tag{11}$$

The assumption of N prime guarantees that they are in $\mathbb{Z}_N$, and the assumption of $p \neq p'$ and a nonzero p guarantees the mapping to be invertible. The indices p, p' make explicit the dependence on p and p' in the definition of $\tilde{\sigma}$ and $\tilde{\mu}$.

We thus find two decoupled Z_N clock models

$$-\beta\mathscr{H}_{p,p'} = \sum_i \sum_{j\sim i} \left(K_1 \tilde{\sigma}_{i;p} \tilde{\sigma}_{j;p}^{-1} + K_2 \tilde{\mu}_{i;p'} \tilde{\mu}_{j;p'}^{-1}\right), \tag{12}$$

one in the composite variable $\tilde{\sigma}_p$ and the other in the composite variable $\tilde{\mu}_{p'}$. Now, we suppose that the couplings are such that one of the two variables, say $\tilde{\sigma}_p$, is ordered (recall that if N is prime, $\mathbb{Z}_N$ models can have only a single symmetry-broken phase), and that μ is disordered. Notably, since $\tilde{\mu}_{p'} = \mu\sigma^{p'}$ this also implies that $\tilde{\mu}_{p'}$ is disordered for all $p' \neq p$. We then claim that under these conditions the model is in a "topological phase of type p." Three questions need to be answered to justify

this statement: (i) Why is this a phase? (ii) Why do different p's correspond to distinct phases? (iii) Why are they topological?

Considering the first point, note that the hidden order of the σ variables manifested by order in $\tilde{\sigma}_p$ is a robust property. Indeed, as argued in the previous case of an Ising symmetry, any local symmetric and defect-free perturbation in original model would map to a local term in the $\tilde{\sigma}_p$ and $\tilde{\mu}_{p'}$ degrees of freedom. Thus, robustness of the topological phase is implied by the usual robustness of broken-symmetry states. Turning to the second point, and the role of p, we can simply note that two different values of p correspond to two different order parameters and thus two different phases. Indeed, if $\tilde{\sigma}_{i;p}$ is long-range ordered, then $\tilde{\sigma}_{i;p'}$ must be disordered as it is equal to a power of $\tilde{\sigma}_{i;p}$ times a nontrivial power of the disordered variable μ_i.

Lastly, we justify the nomenclature topological. By this we mean that an interface between two distinct admissible phases would contain some form of long-range or quasi-long-range order. Consider such an interface between a p topological phase and a p' topological phase. This scenario can be engineered by setting $K_2 = 0$ and $\tilde{\sigma}_p$ ordered on one side of the interface, and $K_1 = 0$ and $\tilde{\mu}_{p'}$ ordered on the other. On the interface, these two order parameters will leak and so $(\mu_i \sigma_i^p)(\mu_i \sigma_i^{p'})^{-1} = \sigma_i^{p-p'}$ would be ordered. Notably the latter, and only the latter, is a local order parameter and thus we have shown the existence of 1D long-range order on such interfaces.

III. THREE DIMENSIONS

Next, we wish to generalize the above construction to 3D. In 2D we attached closed polygons to domain walls of the spins. Turning to 3D, polygons on the dual lattice appear naturally in $\mathbb{Z}_2$ gauge theories, where they correspond to discrete flux lines. However, domains walls become 2D objects, and we instead look for a property of the spins that can also be described in terms of polygons.

Such a spin quantity has been studied recently in [30,31] and can be thought of as an algebraic generalization of the usual continuum notion of vorticity. Consider a cubic lattice and orient links and plaquettes. Next, place a spin variable $\sigma = \pm 1$ at each vertex. The discrete vorticity ω_p on a plaquette p is defined as

$$\omega_p = \frac{1}{2} \sum_{(ij)\in\partial p} \epsilon_{ij}^p \frac{1-\sigma_i\sigma_j}{2}, \tag{13}$$

where the sum is over links on the boundary of p and $\epsilon_{ij}^p = 1$ if the link is oriented as the plaquette, and -1 otherwise. We remark that $\omega_p = 0, \pm 1$ and the choice of plaquette orientation has no effect on the $\mathbb{Z}_2$ quantity $(-1)^{\omega_p}$ that we consider below. For definiteness, we choose orientations as in Fig. 3.

An intuitive view on discrete vorticity comes form thinking of the spins $\sigma_i = +1, -1$ as the elements 0,1 in $\mathbb{Z}_2$. Then, ω_p appears as the discrete integral (i.e., a sum) around a plaquette over the discrete derivatives $\frac{1}{2}(1-\sigma_i\sigma_j) \in \mathbb{Z}_2$. Here, it is important to interpret the discrete derivative as a variable in $\mathbb{Z}$ rather than in $\mathbb{Z}_2$, and hence this sum can be nonzero multiple of $|\mathbb{Z}_2| = 2$. This is analogous to what one does when calculating vorticity of a U(1) variable (ϕ) where derivatives ($i\phi^{-1}\partial_l\phi$) are taken in U(1) but then integrated over as elements in $\mathbb{R}$ whose sum can now be a nonzero multiple of 2π.

In analogy with usual vorticity, the discrete vorticity obeys a discrete version of the zero divergence constraint: given any box on the square lattice, $\sum_{p\in\text{box}} \omega_p = 0 \mod 2$. This can be shown by noting that for each box we can choose a clockwise orientation (when looking from inside the box) on each plaquette. Consequently, each link on the box would appear exactly twice with opposite values of ϵ_{ij}^p. Therefore, discrete vorticity lines form polygons on the dual lattice which obey the exact same branching rules as fluxes in a $\mathbb{Z}_2$ gauge theory.

Tools from lattice gauge theory, specifically cellular and simplicial cohomology, shed further light on this quantity. A thorough discussion of these aspects is relegated below in Sec. III C 1 where they will be used to define discrete vorticity for other Abelian groups.

Armed with the notion of discrete vorticity and its properties, we can now introduce the 3D model. Consider spins σ_i on the vertices of a cubic lattice and $\mathbb{Z}_2$ gauge variables A_{ij} on the links, and choose the following energy:

$$-\beta\mathscr{H} = J_1 \sum_p (AAAA)_p + J_2 \sum_p (-)^{\omega_p} (AAAA)_p, \tag{14}$$

with $(AAAA)_p$ being the product of the four A_{ij} surrounding the plaquette p.

In analogy with our 2D analysis, we would now want to perform some nonlocal transformation to decouple the gauge variables from the spins. Even though both flux and vorticity lines form closed polygons, the number of distinct flux configurations, which spans all such polygons, is bigger than that of vorticity configurations which only span a subset. Therefore, for any vorticity there exists a matching flux although the converse is not true. It follows that there exists A_σ such that $(A_\sigma A_\sigma A_\sigma A_\sigma)_p = (-)^{\omega_p}$. Defining $\tilde{A} = AA_\sigma$, we obtain

$$-\beta\mathscr{H} = J_1 \sum_p (-)^{\omega_p} (\tilde{A}\tilde{A}\tilde{A}\tilde{A})_p + J_2 \sum_p (\tilde{A}\tilde{A}\tilde{A}\tilde{A})_p. \tag{15}$$

There are two points in phase space where the gauge and spin degrees of freedom decouple. The trivial case is $J_2 = 0$ which implies free σ's and a standard $\mathbb{Z}_2$ gauge theory for the A's. For $J_1 > J_c$, where $J_c = 0.762(2)$ is the critical temperature of the dual Ising model on the cubic lattice, the gauge theory has a perimeter law for Wilson loops and linearly confines monopoles (open flux lines), but deconfines static charges of the gauge field [27]. The nontrivial case is $J_2 > J_c$ and $J_1 = 0$ and has the same confining bulk physics only in the composite gauge variable $\tilde{A}$. Notably, the transformation $\tilde{A} = AA_\sigma$ can be viewed as acting on the flux degrees of freedom by multiplying them with vorticity lines. Since vorticity lines consist of closed polygons, this transformation leaves the monopole configuration unchanged. Consequently, the nontrivial phase also confines monopoles. See Fig. 2 for a representation of the nontrivial phase.

The above CTP is a robust phase of matter. As in the 2D model, the nonlocal transformation $\tilde{A} = AA_\sigma$ maps local symmetric and gauge symmetry respecting operators, into

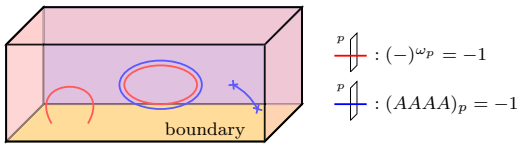

FIG. 2. Pictorial representation of low-energy configurations of the 3D classical topological paramagnet. Along red (blue) lines the discrete vorticity of the spins (the gauge flux) is nonzero. In the bulk, both of these lines must form closed paths. Energetically, they are also encouraged to pair up (middle shape). At a boundary (bottom, orange) the flux is zero but vorticity lines may end. Since a closed flux loop cannot follow an open vorticity line, frustration occurs implying linear confinement of surface vortices. The opposite effect occurs for monopoles of the gauge field (crosses), leading again to linear confinement.

local ones, and leaves the free energy invariant. Respecting these symmetries, both the monopole confining phases of $\tilde{A}$ and A are well-defined phases [32]. In addition, we found that breaking the gauge symmetry on an interface or boundary does not destroy the surface physics (see below), suggesting that gauge symmetry is not crucial here.

A. Surface theory

To establish the distinction between trivial and nontrivial phases and to support this nomenclature, we now discuss an interface. For concreteness, we take coordinates $(x,y,z) \in \mathbb{Z}^3$ for the vertices of the lattice and identify the interface as the $x = 0$ plane. We also denote P_L (P_R) the plaquettes in the region $x \leqslant 0$ ($x > 0$). In the limit $J_2, J_1 \to \infty$, $(AAAA)_{\tilde{p}} = 1$ for $\tilde{p} \in P_R$. By conservation of flux, we find that for all boundary plaquettes $p \in \partial P$, $(AAAA)_p = 1$. Consequently, since J_2 forces $(-)^{\omega_p}(AAAA)_p = 1$, $\omega_p = 0$ on the 2D boundary. The surface partition function in this limit is thus given by

$$Z_{\text{surf},0} = \sum_{\sigma} \prod_{p\in\partial P} \delta(\omega_p) = \sum_{\sigma,\tau} \prod_{p\in\partial P} (\tau)^{\omega_p}. \tag{16}$$

The possible domain-wall configurations for σ's in 2D are depicted in Fig. 3 where a second mapping to arrow configurations of the eight-vertex model is also discussed.

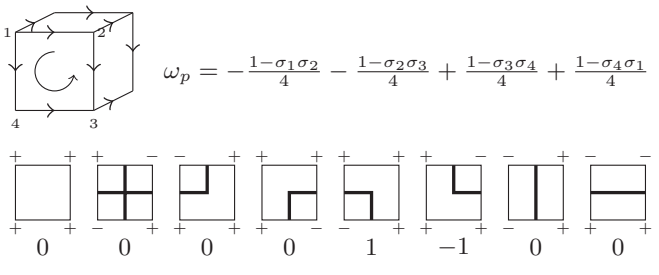

FIG. 3. (Top) Choice of orientations of links and the formula for ω_p for the front face. (Bottom) σ domain-wall configurations together with their ω_p values. Domain-wall configurations are in bijection with arrow configurations of the eight-vertex model by associating up/down (right/left) arrows on vertical (horizontal) links with presence/absence of thick lines.

The constraint $\omega_p = 0$ implies a two-in–two-out ice rule, supporting the vorticity interpretation and mapping the surface theory to the critical six-vertex model with an anisotropy parameter $\Delta = \frac{1}{2}$ [33].

The latter model is critical and described by a compact free boson ϕ. This fact can be established with the Coulomb gas method [34], which we now briefly recall. Denoted by $S_\ell = \pm 1$ the arrow at link ℓ, note that S is conserved around a vertex, and one can introduce a height field $h(i)$ on the same sites where σ lives, such that h increases by π in crossing an arrow pointing up from the right. This discrete height renormalizes at long distances to a Gaussian free field, a conformal field theory with central charge $c = 1$, and via this mapping one can compute dimensions of operators. Noting that $\sigma_i\sigma_j = \prod_{\ell\in\Gamma_{ij}} -ie^{i\pi S_\ell/2} \propto e^{ih(i)/2}e^{-ih(j)/2}$, σ is found to have scaling dimension $\frac{3}{8}$. Similarly, noting that the two-point function of τ in Eq. (16) corresponds to inserting two vortices where the height field has discontinuity of $\pm 4\pi$, τ has dimension $\frac{2}{3}$. Identifying $\phi \equiv h/2$, one has the effective theory

$$\mathscr{L} = \frac{g}{4\pi}(\nabla\phi)^2, \quad g = \frac{4}{3}. \tag{17}$$

The appearance of half-integer electric charges follows also naturally by considering the torus partition function. Indeed, on $4L \times 4L'$ lattices, periodic boundary conditions for the σ's select only even frustrations for the height field as it winds around a cycle, resulting in half-integer electric charges and even magnetic charges. Microscopically, σ is a Hermitian linear combination of $e^{\pm i\phi}$ and τ of $e^{\pm i\theta}$, θ being the dual field. Therefore, the symmetry is realized as anticipated in the main text: $\phi \to \phi + \pi$ and $\theta \to \theta + \pi$, as it does in quantum SPTs [35,36]. We also note that even though the local weight (16) has no such symmetry, the global weight still has it, due to the global constraint $\prod_p (-1)^{\omega_p} = 1$ for a closed manifold. From this analysis it follows that the lattice $\mathbb{Z}_2 \times \mathbb{Z}_2$ symmetry is realized in the field theory in an anomalous chiral way: $\phi \to \phi + \pi$ and $\theta \to \theta + \pi$, where θ is the dual field.

Let us consider perturbations to this surface model. Adding a $\sigma\sigma$ term to the boundary action corresponds to the six-vertex model in an external field. Denoted by $H/2$ and $V/2$ the horizontal and vertical couplings, the theory remains critical within the region $(e^{2|H|} - 1)(e^{2|V|} - 1) \leqslant 1$ [37], the only effect of $H, V \neq 0$ being renormalizing the stiffness of ϕ [38]. A ferromagnetic coupling between the τ's would generically induce the RG-irrelevant term $\cos(2\theta)$. Interestingly, the relevant $\cos(\theta)$ term is forbidden without requiring any fine tuning of the couplings. Formally, it is because of the emergent $\mathbb{Z}_2 \times \mathbb{Z}_2$ symmetry. Physically, it is because $\pm 2\pi$ vortices are linearly confined by the bulk (see Fig. 2). Further, a gauge symmetry-breaking term $(K \sum_{\ell\in\partial E} A_\ell)$ can also be studied using duality [39] and has no effect on the σ's in the limit $J_2, J_1 \to \infty$.

B. SPT perspective

As discussed in Sec. II A, the $\mathbb{Z}_2 \times \mathbb{Z}_2$ two-dimensional classical topological paramagnet can be related to the imaginary-time partition function of a $(1 + 1)$D quantum SPT phase. In this section we provide support for the analogous

statement in 3D, proving that all of the above models are in the same universality class as the Euclidean time partition function of certain $(2+1)$D quantum SPTs. We will show this by analyzing the responses to gauge fluxes or, equivalently, the statistical phases obtained by braiding flux excitations.

As starting point we perform a gauge-to-Ising duality transformation on the bulk [39] trading A's for spins τ's on the vertices of the dual lattice, resulting in an equivalent bulk theory with weights:

$$\prod_{p\in P_L}(\tanh J_2)^{\frac{1-\tau_k\tau_l}{2}}\prod_{p\in P_R}(\tanh J_1)^{\frac{1-\tau_k\tau_l}{2}}(\tau_k\tau_l)^{\omega_p}, \tag{18}$$

where kl is the link dual to p. The term $\prod_{p\in P_R}(\tau_k\tau_l)^{\omega_p}$ is in fact topological. It is always one in a geometry without interfaces since then vorticity lines where $\omega_p=\pm1$ form polygons, and in the product of $\tau_k\tau_l$ along each such polygon, each τ appears an even number of times, and hence the product is always one. Focusing on the analytically tractable case of $J_1=0$ leaves us with the partition function

$$Z=\sum_{\tau,\sigma}\prod_p e^{\tilde{J}_2\tau_k\tau_l}(\tau_k\tau_l)^{\omega_p}, \tag{19}$$

where $\tilde{J}_2=\frac{1}{2}\ln[\tanh(J_2)]$, and here and below (kl) is the link dual to the plaquette p. Since this model now has a $\mathbb{Z}_2\times\mathbb{Z}_2$ symmetry, it is natural to seek a quantum counterpart which utilizes such a symmetry, and these are known as type ii SPT phases [8,40,41]. These SPTs are characterized by a quantized bulk response to static gauge fluxes. For a $\mathbb{Z}_2\times\mathbb{Z}_2$ symmetry, a π Ising flux for one symmetry would attract a fractional symmetry charge of the other symmetry. This is the discrete analog of flux attachment in the integer quantum Hall effect, where a π flux would attract half an electron charge [42]. If our model belongs to the same phase as that described by the imaginary-time partition function of one of such $(2+1)$D SPTs, it should exhibit the same flux responses.

We therefore introduce two additional static gauge fields (B^σ,B^τ) which are coupled to matter in the usual manner: we trade each $\tau_k\tau_l$ with $\tau_k B^\tau_{kl}\tau_l$ and each $\sigma_i\sigma_j$ with $\sigma_i B^\sigma_{ij}\sigma_j$. The adjective static refers to the fact that they are not summed over in the partition function, which is then

$$Z(\{B^\tau\},\{B^\sigma\})=\frac{1}{Z}\sum_{\tau,\sigma}\prod_p e^{\tilde{J}_2\tau_k B^\tau_{kl}\tau_l}\left(\tau_k B^\tau_{kl}\tau_l\right)^{\omega_p(B^\sigma)}, \tag{20}$$

where $Z\equiv Z(\{1\},\{1\})$ as above. If we require that both fluxes are zero everywhere, namely $\prod_{(ij)\in\partial p}B^\sigma_{ij}=\prod_{(kl)\in\partial p^*}B^\tau_{ij}=1$, where p^* is a dual plaquette, we can rewrite $B^\sigma_{ij}=\tilde{\sigma}_i\tilde{\sigma}_j$, $B^\tau_{kl}=\tilde{\tau}_k\tilde{\tau}_l$, and reabsorb the B's in the definition of σ,τ. Thus, introducing gauge fields with zero flux is equivalent to set them to 1. When coupling to gauge fields, from formula (5) of the main paper the vorticity becomes

$$(-)^{\omega_p(B^\sigma)}=\prod_{(ij)\in\partial p}\exp\left(i\pi\frac{1-\sigma_iB^\sigma_{ij}\sigma_j}{4}\epsilon^p_{ij}\right). \tag{21}$$

If we now violate the zero-flux constraint, then $(-)^{\omega_p(B^\sigma)}$ can assume the additional values $\pm i$ on top of ±1 which it had before. A related issue to be discussed is the definition of plaquette orientations which enter the sign ϵ^p_{ij}. Changing plaquette orientations corresponds to change the exponent of (21) by an overall sign. For zero B^σ flux, this choice is immaterial; however, in the case of π flux it does matter. For definiteness, we choose to orient both links and their dual as the positive direction of the axis of three-dimensional space they are parallel to, and adopt a left-hand rule for defining clockwise/anticlockwise plaquette orientations.

The topological quantity we wish to calculate concerns the flux responses in type ii SPT phases with a $\mathbb{Z}_2\times\mathbb{Z}_2$ symmetry and we now recall its definition. Consider then a quantum SPT model with $\mathbb{Z}_2\times\mathbb{Z}_2$ symmetry on a two-dimensional lattice, and denote by $\sigma^{x,z},\tau^{x,z}$ the elementary spin operators, and by $|\mathrm{gs}\rangle$ its ground state. It can be shown [40] that the insertion of a π flux associated with one of the symmetries draws in a fractional symmetry charge associated with the other symmetry. To probe this, we introduce two B^τ π fluxes into the system by creating them and taking them apart at positions a,b. Note that these excitations are stringlike and a string will be attached to these two fluxes. Their world lines draw a surface S_1 in space-time whose interior is swiped by the string. The system is then let to evolve until it reaches its new ground state, and we denote the operator that performs this operation by π_{ab}. Further, we denote by S_2 the set of vertices on a region surrounding only one of the fluxes and choose this region to be larger than the correlation length.

The operator $\rho_{S_2}=\prod_{i\in S_2}\sigma^x_i$ can be interpreted in two ways. First, as creating, evolving, and annihilating two B^σ π fluxes along the boundary of S_2. Second, as a measurement of the local Ising charge around just one flux. In a nontrivial type ii SPT with a $\mathbb{Z}_2\times\mathbb{Z}_2$ symmetry, the ratio $\langle\mathrm{gs}|\pi^\dagger_{ab}\rho_{S_2}\pi_{ab}|\mathrm{gs}\rangle/\langle\mathrm{gs}|\rho_{S_2}\pi^\dagger_{ab}\pi_{ab}|\mathrm{gs}\rangle$ should be equal to $\pm i$ [40], the sign depending on which of the two B^τ fluxes is encircled by S_2. According to the previous discussion, one can view this as the phase associated with braiding the two flux excitations (in similar spirit to Ref. [43]) or alternatively as a generalization of Laughlin's pumping argument to discrete symmetry as the π flux draws in half an Ising symmetry charge (recall that in this multiplicative notation, an Ising charge is -1 and so half a charge is $\pm i$).

Upon switching to imaginary time, the quantum mechanical overlaps making up this ratio can be reformulated as partition functions. The factor $\langle\mathrm{gs}|\pi^\dagger_{ab}\rho_{S_2}\pi_{ab}|\mathrm{gs}\rangle$ is illustrated in Fig. 4(a), where across the S_1 surface (blue) the interaction between the τ's is reversed and across the S_2 surface (green)

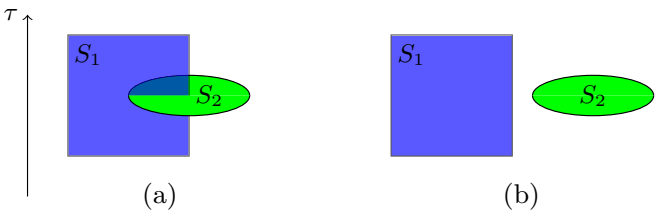

FIG. 4. Partition function formulation of the generalized Laughlin's argument or equivalently the braiding of two π fluxes. Across the square blue surface S_1 the sign of the interaction between two τ's is reversed. Similarly, across the oval green surface S_2 the sign of the interaction between two σ's is reversed. The ratio between these two partition function equals $\pm i$ for the nontrivial type ii SPT with a $Z_2\times Z_2$ symmetry.

the interaction between the σ's is reversed. As in the main text, links where the interaction is reversed are referred to as frustrated. The factor $\langle \mathrm{gs}|\rho_{S_2}\sigma_i^x\pi_{ab}^\dagger\pi_{ab}|\mathrm{gs}\rangle$ illustrated in Fig. 4(b) contains the same two elements, however, now these are separated in imaginary time. More specifically, let us denote by G and G^* the lattice and its dual, where σ and τ, respectively, live. As defined, S_1 and S_2 will be a connected region of G and G^* (note the order of G and G^*) across which the τ and σ couplings, respectively, are reversed. By a region here we mean a set of neighboring plaquettes and links around them on both the interior and the boundary of the region. Since it will be clear from the context, we we will write $(kl) \in S_2$ for links in the region S_2. Further, ∂S_i will denote the set of links on the boundary of S_i. We remark that frustrated links intersecting S_1 (S_2) correspond to introducing a B^τ (B^σ) π flux on the plaquettes intersecting ∂S_1 (∂S_2), consistently with the above discussion.

Before delving into the details of calculating the relevant ratio, let us give a physical picture supporting why it would come out purely imaginary. In the presence of nontrivial fluxes, the relation $\sum_{p\in\mathrm{box}}\omega_p(B^\sigma)=0 \mod 2$ does not hold in general. Instead, one has an altered Z_4 zero-divergence relation given by $2[\sum_{p\in\mathrm{box}}\omega_p(B^\sigma)O_p^{\mathrm{box}}]=0 \mod 4$, where $O_p^{\mathrm{box}}=1$ (-1) if the plaquette's orientation appears as clockwise (anticlockwise) when viewed from within the box. Using this new relation, one may show that the vorticity line configuration in the presence of the B^σ flux loop contains a single fractional vorticity line encircling S_2 as well as other fluctuating integer vorticity lines. Given the form of the topological term, the integer vorticity lines cannot contribute imaginary factors and so we may put them aside for now. Considering the fractional vorticity line, if it does not cross S_1 [case (b)], the term $\Pi_{(kl)\in\partial S_1}(\tau_k\tau_l)$ is equal to 1. Consequently, the topological term, which involves a fractional power of this product, cannot give an imaginary contribution. On the other hand, if this fractional vorticity line crosses S_1 [case (a)], this product would be -1, and the topological term would be purely imaginary.

We now substantiate the above argument with some simple and exact computations. First, notice that there are four cases to consider for the weight $w(kl)$ per dual link (kl), in case frustrations for both τ and σ are present:

$$w(kl)=\begin{cases} e^{\tilde{J}_2\tau_k\tau_l}(\tau_k\tau_l)^{\tilde{\omega}_p}, & (1): kl\in S_2,\ \not\cap S_1\\ e^{-\tilde{J}_2\tau_k\tau_l}(-\tau_k\tau_l)^{\tilde{\omega}_p}, & (2): kl\in S_2,\cap S_1\\ e^{-\tilde{J}_2\tau_k\tau_l}(-\tau_k\tau_l)^{\omega_p}, & (3): kl\notin S_2,\cap S_1\\ e^{\tilde{J}_2\tau_k\tau_l}(\tau_k\tau_l)^{\omega_p}, & (4): kl\notin S_2,\ \not\cap S_1 \end{cases} \tag{22}$$

where $\tilde{\omega}_P$ corresponds to $\omega_p(B^\sigma)$ with frustrated links where $B^\sigma=-1$. Defining the set of couplings

$$\hat{B}_\ell^\tau=\begin{cases}-1 & \ell\cap S_1\\ 1 & \ell\not\cap S_1\end{cases},\quad \hat{B}_\ell^\sigma=\begin{cases}-1 & \ell\cap S_2\\ 1 & \ell\not\cap S_2\end{cases}, \tag{23}$$

the observable of interest is

$$\begin{aligned} Z(\{\hat{B}^\tau\},\{\hat{B}^\sigma\}) &= \frac{1}{Z}\sum\prod_{kl\in S_2,\not\cap S_1} e^{\tilde{J}_2\tau_k\tau_l}(\tau_k\tau_l)^{\tilde{\omega}_p}\\ &\quad\times\prod_{kl\in S_2,\cap S_1} e^{-\tilde{J}_2\tau_k\tau_l}(-\tau_k\tau_l)^{\tilde{\omega}_p}\\ &\quad\times\prod_{kl\notin S_2,\cap S_1} e^{-\tilde{J}_2\tau_k\tau_l}(-\tau_k\tau_l)^{\omega_p}\\ &\quad\times\prod_{kl\notin S_2,\not\cap S_1} e^{\tilde{J}_2\tau_k\tau_l}(\tau_k\tau_l)^{\omega_p} \end{aligned} \tag{24}$$

$$\begin{aligned} &= \frac{1}{Z}\sum\prod_{kl\cap S_1} e^{-\tilde{J}_2\tau_k\tau_l}(-\tau_k\tau_l)^{\omega_p}\\ &\quad\times\prod_{kl\not\cap S_1} e^{\tilde{J}_2\tau_k\tau_l}(\tau_k\tau_l)^{\omega_p}\prod_{kl\in S_2}(\tau_k\tau_l)^{\tilde{\omega}_p-\omega_p}\\ &\quad\times\prod_{kl\in S_2,\cap S_1}(-1)^{\tilde{\omega}_p-\omega_p}. \end{aligned} \tag{25}$$

At this point, we use the following identity:

$$\prod_{kl\in S_2}(\tau_k\tau_l)^{\tilde{\omega}_p-\omega_p}=1. \tag{26}$$

To prove it, first notice that given the choice of orientation described in the text above, $\tilde{\omega}_p-\omega_p$ gives a factor $\epsilon_{ij}^p\sigma_i\sigma_j/2$ per frustrated link ij. Then, group together all τ's having a given exponent $\sigma\sigma'/2$. τ's appear in pairs for any choice of bond $\sigma\sigma'$, and cancel either because $\tau^2=1$ or because $\tau\tau^{-1}=1$.

We now rewrite the partition function in terms of the original A gauge degrees of freedom to take advantage of the change of variables $A\to\tilde{A}$ as in Eq. (15), which decouples gauge and spin degrees of freedom. Reversing the couplings along S_1 for the τ's corresponds in the A language to computing the Wilson loop along the perimeter of S_1 (see, e.g., [29]), so that one has

$$\begin{aligned} &Z(\{\hat{B}^\tau\},\{\hat{B}^\sigma\})\\ &\quad= Z^{-1}\sum\prod_{p\in S_1}(AAAA)_p\\ &\qquad\times\prod_p e^{J_2(AAAA)_p(-)^{\omega_p}}\prod_{p\in S_1,\cap S_2}(-1)^{\tilde{\omega}_p-\omega_p} \end{aligned} \tag{27}$$

$$= \left\langle\prod_{\ell\in\partial S_1}\tilde{A}_\ell\right\rangle_{\tilde{A}}\left\langle\prod_{p\in S_1}e^{i\pi\omega_p}\prod_{p\in S_1,\cap S_2}e^{i\pi(\tilde{\omega}_p-\omega_p)}\right\rangle_\sigma, \tag{28}$$

where the average $\langle\dots\rangle_{\tilde{A}}$ is taken with the partition function of $\tilde{A}$'s alone, and the average $\langle\dots\rangle_\sigma$ is taken with the trivial partition function for the σ's that gives a weight of 1 to each σ configuration. The last term in the σ expectation values involves the links illustrated in Fig. 5.

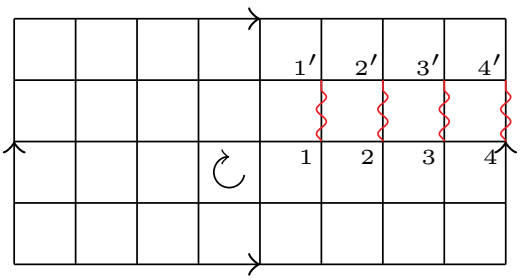

FIG. 5. The surface S_1. Red bonds are those which intersect S_2 and are frustrated in the σ variables.

Due to cancellations on the internal edges, now we have the following identities [recall also the discussion around (26), and use the notation of sites along the frustrations as in Fig. 5]:

$$\prod_{p\in S_1} e^{i\pi\omega_p} = \prod_{(ij)\in\partial S_1} i^{\epsilon(ij)^p \frac{1-\sigma_i\sigma_j}{2}}, \tag{29}$$

$$\prod_{p\in S_1,\cap S_2} e^{i\pi(\tilde{\omega}_p-\omega_p)} = 1 \text{ if (b)} : S_1\cap S_2 = \emptyset, \tag{30}$$

$$\prod_{p\in S_1,\cap S_2} e^{i\pi(\tilde{\omega}_p-\omega_p)} = e^{i\frac{\pi}{2}(-\sigma_1\sigma_1'+\sigma_1\sigma_1'-\sigma_2\sigma_2'+\sigma_3\sigma_3'-\sigma_3\sigma_3'+\sigma_4\sigma_4')} \tag{31}$$

$$= e^{i\frac{\pi}{2}\sigma_4\sigma_4'} \text{ if (a)} : S_1\cap S_2 \neq \emptyset. \tag{32}$$

Therefore, in both (a) and (b) cases, the σ expectation value reduces to a one-dimensional classical spin chain along ∂S_1 which can be easily solved via transfer matrix. The presence of frustration in case (a) corresponds to introducing a twist by the matrix $e^{i\frac{\pi}{2}\sigma\sigma'}$. Under the assumption of a rectangular perimeter ∂S_1 of length $2N$, with the branching structure as in Fig. 5, the σ expectation value in the (a) case is (setting $\sigma_{2N+1}\equiv\sigma_1$)

$$\left\langle \prod_{p\in S_1} e^{i\pi\omega_p} \prod_{p\in S_1,\cap S_2} e^{i\pi(\tilde{\omega}_p-\omega_p)} \right\rangle_\sigma = 2^{-|\partial S_1|}\,\mathrm{Tr}\left[\begin{pmatrix} i & -i \\ -i & i\end{pmatrix}\begin{pmatrix}1 & i\\ i & 1\end{pmatrix}^N\begin{pmatrix}1 & -i\\ -i & 1\end{pmatrix}^N\right] \tag{33}$$

$$= i2^{1-N}. \tag{34}$$

Let us remark that the problem has a chirality given by the branching structure. If S_2 crossed S_1 on the left boundary instead of on the right, the twist matrix would have been $e^{-i\frac{\pi}{2}\sigma\sigma'}$, and it would have produced an extra minus sign. If the flux arrangement is as in Fig. 4(b), the only difference in the result is the absence of the twist matrix appearing first in the above trace. The sole net effect of this is to remove the i factor and therefore the desired ratio is

$$Z^{(a)}/Z^{(b)} = \pm i, \tag{35}$$

depending if S_2 crosses S_1 on its right (+) or left (−). We have thus shown that our model has the same response to π fluxes as the related quantum SPT phase.

C. Generalizations

As done in Sec. II B for the 2D case, we now sketch generalizations of the 3D model beyond the case of a $\mathbb{Z}_2$ symmetry.

1. Discrete vorticity and cellular cohomology

We first address the mathematical description of the discrete vorticity in terms of cellular cohomology which allows for its generalization. We will then outline a classification of CTPs within this framework and analyze some specific models.

Simplicial and cellular cohomology are toolboxes used in lattice gauge theories (see, e.g., [26].). The first requires us to work strictly with simplexes while the second permits more general types of cells, in particular the cubic lattice. Let us quickly describe the necessary mathematical details. A reader interested in only the generalized definition of the discrete vorticity for $G = Z_N$ may skip directly to Eq. (38).

We denote the sets of sites, edges, plaquettes, and boxes of the cubic lattice by V,E,P,B, respectively, and call their elements alternatively 0, 1, 2, and 3 cells. In the obvious manner, each of these sets describes the boundary of the latter one. The relations between cells and their boundaries can be captured in several ways: one is using incidence numbers, where $[a:b]$, with a a d cell and b a $d+1$ cell. These take three possible integer values, $-1,0,1$, which satisfy sum rules, such as $\sum_{e\in E}[v:e][e:p]=0$, $\sum_{p\in P}[e:p][p:b]=0$. Alternatively, one can simply orient the edges and plaquettes and then $[v:e]$ will be 0, 1, or -1 if v is not a boundary of e, v is at the end of e, or v is at the beginning of e. Similarly, $[e:p]$ is 0 if e is not an edge of p, 1 if e is aligned along the orientation of p, or -1 if it is opposite. One can easily verify that these definitions satisfy the sum rules.

Below we use $i,j,k,\ldots$ for vertex indices, $\epsilon_{ij}=1$ (-1) if the edge ij is oriented from i to j (j to i) and $\epsilon^p_{ij}=1$ (-1) if the edge ij is oriented along the orientation of the plaquette (against it).

To define a cellular cohomology structure (or physically a gauge theory coupled to matter), the following steps are needed: First, we pick an Abelian group (the gauge group) G and call an assignment $g: V\to G$ a 0-cochain (matter field), $A: E\to G$ a 1-cochain (gauge field), and $F: E\to G$ a 2-cochain (curvature/flux field). We denote the set of d-cochains by C^d. The coboundary operator δ (see Ref. [26]) maps C^d to C^{d+1}, and is nilpotent, $\delta^2=0$. In particular, $(\delta g)_{ij\in E} = g_i g_j^{-1}$, where the order of ij is chosen according to the orientation of the edge, is the trivial 1-cocycle. [If G is a generic Abelian group, we will use the notation $(\delta g)_{ij}=g_i-g_j$, and if $G=\mathbb{Z}_2$, $g_i=(1-\sigma_i)/2$, where $\sigma_i=\pm1$ is the variable used in the main text.] In general, given $\alpha\in C^d$, $\beta=\delta\alpha$ is a trivial $(d+1)$-cochain, and if $\beta=0$, then α is called a d-cocycle. Next, one can define an equivalence relation where two d-cocycles are equivalent if they differ by a trivial d-cochain: $\alpha_1-\alpha_2=\delta\gamma$, with $\gamma\in C^{d-1}$. The equivalence classes of d-cocycles then obey a group structure known as the d cohomology group $H^d(G)$.

We consider now an exact sequence of Abelian groups of the type

$$0\to G\xrightarrow{f}\tilde{G}\xrightarrow{h}G\to 0, \tag{36}$$

and construct the map $B=f^{-1}\delta h^{-1}$, which is applied to a trivial 1-cocycle δg to produce a 2-cocycle. The map B is called a Bockstein homomorphism [44,45] and is well defined given h^{-1}, f^{-1}. Further, it maps d-cocycles to $(d+1)$-cocycles and introduces a homomorphism between $H^d(G)$ and $H^{d+1}(G)$. In physical terms, it maps a matter configuration to gauge flux configurations with no monopoles.

In general, there are a variety of exact sequences one can consider and hence a variety of Bockstein homomorphisms. These can be classified by classifying the exact sequences upon which they are based. Short exact sequences of the form (36) involving Abelian groups are equivalent to central

extension of G by G (s.t. $G=\tilde{G}/G$). The trivial extension is defined by $\tilde{G}=G\times G, f(a)=(a,0)$ and $h[(a,b)]=b$. Nontrivial extensions are classified by the second group cohomology $H^2(G,G)$. For $G=Z_N$ with N prime, one finds that $H^2(Z_N,Z_N)=Z_N$ and so N distinct choices of discrete vorticity exist.

If we specify to $G=\mathbb{Z}_2$, $\tilde{G}=\mathbb{Z}_4$, and $f(a)=2a$, $h(a)=a \mod 2$, the Bockstein homomorphism B produces precisely $\omega_p \mod 2$ and the 2-cocycle condition implies zero divergence. Moreover, since B is a homomorphism and δg is a trivial 1-cocycle, the 2-cocycle must be trivial as well and hence there exists a 1-cochain (a gauge field A) such that $\delta A=\omega_p$.

We can now use B to define discrete vorticities for other Abelian groups. Consider, for instance, the case $G=\mathbb{Z}_N$, N prime, $\tilde{G}=Z_{N^2}$, and

$$f(a)=Na, \quad h_\ell(a)=\ell a \bmod N, \quad \ell=0,1,\ldots,N-1. \tag{37}$$

Each choice of ℓ realizes one of the N nonequivalent central extensions of $\mathbb{Z}_N$ by $\mathbb{Z}_N$, and leads to a different Bockstein homomorphism with $\ell=0$ being the trivial case. Setting $B_\ell=f^{-1}\delta h_\ell^{-1}$ yields a discrete vorticity generalizing Eq. (13):

$$\omega_p^{(\ell)}=\frac{1}{N}\sum_{(ij)\in\partial p}\epsilon_{ij}^p \ell(g_i-g_j) \mod N^2, \tag{38}$$

where i and j in the above are chosen such that i (j) is at the start (end) of the edge $(\vec{ij})$ and $\epsilon_{ij}^p=1$ (-1) if the edge is oriented with (against) the plaquette p. {Equivalently, ϵ_{ij}^p is the incidence number $[(\vec{ij}):p]$ in the notation of Ref. [26].} Explicitly, referring to Fig. 3, it reads as

$$\omega_p^{(\ell)}=\frac{1}{N}(\ell(-(g_1-g_2)-(g_2-g_3)+(g_4-g_3)+(g_1-g_4)) \mod N^2). \tag{39}$$

The nontriviality of this expression is due to the fact that the terms (g_i-g_j) are understood in $\mathbb{Z}_N$.

Lastly, we comment on the connection between the above cellular-cohomology approach and the group-cohomology approach to SPTs [8]. Quantum SPTs at $d+1$ spatial dimensions with a symmetry Q are classified by the group-cohomology group $H^{d+1}(Q,U(1))$. In our classical context, $d+1$ is actually the overall dimension, and so one may expect that our phase is contained in $H^3(Q,U(1))$. If our matter fields possess a Z_N symmetry and the gauge symmetry is Z_N, the relevant symmetry group in our context is $Q=Z_N\times Z_N$. (This is shown explicitly in the next section for $N=2$.) Considering $Q=Z_N\times Z_N$, the Kunneth formula [28] tells us that $H^3(Z_N\times Z_N,U(1))=\mathbb{Z}_N^3$ contains $H^2(Z_N,H^1(Z_N,U(1)))=H^2(Z_N,Z_N)$ which is also the quantity which classifies central extensions, as discussed above. It would be interesting to find the exact correspondence between $H^3(G\times G',U(1))$ and possible CTPs. In particular, find out whether every element in $H^3(G\times G',U(1))$ corresponds to a classical (or local sign-free) partition function.

2. *Discrete vorticity models of 3D CTPs with $G=G'=\mathbb{Z}_N$*

Using the above definition of a discrete vorticity for $G=Z_N$ one can readily define more general models of 3D CTPs. To this end, we consider a cubic lattice with vertices indexed by i, oriented edges pointing from i to j by (ij), and oriented plaquettes indexed by p. The model has $\sigma_i\in\mathbb{Z}_N$ degrees of freedom on vertices and $A_{ij}\in\mathbb{Z}_N$ degrees of freedom on edges of the lattice. As in the two-dimensional case, $\mathbb{Z}_N$ degrees of freedom take values in the roots of unity ($e^{2\pi i\alpha/N}$). (However, we still represent $\omega_p^{(\ell)}$ as a number between $0,\ldots,N-1$.) In this notation, the generalized model is given by

$$-\beta\mathscr{H}=\sum_p J_{\ell'}e^{\frac{2\pi i\omega_p^{(\ell')}}{N}}(AAAA)_p+\text{c.c.} + \sum_p J_\ell e^{\frac{2\pi i\omega_p^{(\ell)}}{N}}(AAAA)_p+\text{c.c.}, \tag{40}$$

with $\omega_p^{(\ell)}$ being the discrete vorticity from Eq. (38), which depends on g_i defined by $\sigma_i=e^{2\pi i g_i/N}$ and $(AAAA)_p\in\mathbb{Z}_N$ is the product of $A_{ij}^{\epsilon_{ij}^p}$'s along the plaquette p.

First, let us analyze the case when only J_ℓ is nonzero. The previous discussion on $\omega_p^{(\ell)}$ shows that for every σ configuration there is a A_σ configuration such that $(A_\sigma A_\sigma A_\sigma A_\sigma)_p=\omega_p^{(\ell)}$. Thus, going to the composite gauge variable $\tilde{A}=AA_\sigma$ one obtains $-\beta\mathscr{H}=J_\ell(\tilde{A}\tilde{A}\tilde{A}\tilde{A})_p$, a pure $\mathbb{Z}_N$ lattice gauge theory.

Performing a generalized Kramers-Wannier duality [39], a $\mathbb{Z}_N$ lattice gauge theory becomes a 3D clock model with rotor variables taking values in $\mathbb{Z}_N$. For prime N, so that $\mathbb{Z}_N$ does not have any subgroups, the model will exhibit two distinct thermodynamic phases: a disordered phase where the rotors are disordered and an ordered phase of the rotors separated by a second-order phase transition at J_c. In gauge theory terms, these correspond, respectively, to a phase with short flux loops ($J_\ell>J_c$) and one with large flux loops ($J_\ell<J_c$). Following the exact same reasoning as done for the Z_2 case, we find that the former phase confines defects of the constraint and since σ can fluctuate freely, it clearly does not break any symmetry. Consequently, it is an admissible phase in our classification.

We argue that the phase obtained for $J_\ell>J_c$ is a classical topological phase of type ℓ. As discussed previously, it is a phase since local symmetry and gauge respecting perturbation in the σ,A degrees of freedom map to local symmetry and gauge respecting perturbation in the $\sigma,\tilde{A}$ notation and vice versa. Knowing that the latter is a well-defined thermodynamic phase then implies that the former one is well defined as well. To see why different ℓ correspond to distinct phases, let us consider an interface between a phase with large $J_\ell\to\infty, J_{\ell'}=0$ on the left and $J_{\ell'}\to\infty, J_\ell=0$ on the right. At the interface, $\omega_p^{(\ell)}=\omega_p^{(\ell')}$. Now, since $\omega_p^{(\ell)}=\ell\omega_p^{(1)} \mod N$ and N is prime, consistency implies either $\ell=\ell'$ or $\omega_p^{(1)}=0$. Supposing $\ell\neq\ell'$, this shows that just as in the Z_2 case, the boundary is described by a 2D statistical mechanical model where a zero vorticity constraint is imposed on every square. Taking $J_\ell>J_c$ but finite on the left and $J_{\ell'}>J_c$ on the right will result in a physically similar scenario where flux lines crossing the interface are confined to neutral pairs by the bulks. We will argue momentarily that the model with zero vorticity is gapless. This, together with the relations to the group-cohomology classification of the previous section,

strongly suggests that different ℓ correspond to different phases. One way of proving this would be to generalize the arguments of Sec. III B to $\mathbb{Z}_N$, and is left for future work.

Let us analyze the resulting theory on the two-dimensional interface. We first count the number of zero-vorticity constraints at a plaquette. We change variables from site to link variables $s_{ij} = g_i - g_j$, where as before $\sigma_i = e^{2\pi i g_i/N}$. The four link variables around a plaquette can assume only N^3 since a global shift of g_i leaves the link variables unchanged. (In the following, we will ignore the multiplicative factor N in the weight produced by this change of variables.) For the purpose of counting the zero-vorticity configurations, we can ignore this constraint and consider the link variables independent since the missing N configurations have nonzero vorticity. We are thus left with a vertex model, where each link has N states and zero vorticity becomes an interaction at vertices of dual lattice. Further, the zero-vorticity constraint is the same for any ℓ in (38) and w.r.t. the labelings of vertices and orientations as in Fig. 3, it reads as

$$-s_{12} - s_{23} + s_{43} + s_{14} = 0. \tag{41}$$

If the N states are labeled $-S, \ldots, S$, with $S = \frac{N-1}{2}$, this coincides with U(1) invariant configurations of spin-S vertex models, and the resulting number of nonzero configurations is

$$\frac{N}{3}(2N^2 + 1) = 6, 19, 44, 85, \ldots. \tag{42}$$

Apart from the already discussed $N = 2$ case, other values of N may not correspond to integrable weights for the vertex model, as we will discuss now for the case $N = 3$, where the number of vertices is 19. In such case, there are two classes of integrable 19 vertex models, both of which can be related to a loop model (see, e.g., [46]). In particular, our model gives uniform weight one to each vertex and cannot be related to a loop model, at least not in the standard fashion where states of labels ± 1 are associated to oriented strands of loops and states of labels 0 to vacancies. Nonetheless, this model belongs to a class of models studied numerically in relation with Berezinskii-Kosterlitz-Thouless transition in [47], suggesting that the model is critical and with $c = 1$.

IV. CONCLUSION

In this work, we have introduced a topological classification scheme of classical statistical mechanical systems. This involved defining the objects of the classification (admissible phases), the equivalence relations between them (continuous deformation without phase transitions), and lastly showing that the classification is not trivial by giving concrete examples of admissible phases which are inequivalent. We have found N distinct models for CTPs in 2D and 3D for systems with a $\mathbb{Z}_N$ symmetry and defects carrying a $\mathbb{Z}_N$ charge. An important question concerning the ability to identify the topological index or equivalence class given the bulk behavior of a particular model is left for future work.

The CTPs introduced in this work, together with the ones discussed in [24,48], describe, to the best of our knowledge, types of topological classical phases of matter. The models given here are, arguably, the simplest and most minimal ones having just a spin degree of freedom per site and per link. Another salient feature is that they can be simulated using classical Monte Carlo. They may thus serve as a test bed for studying various open questions concerning both classical topological paramagnets and their quantum counterparts [8]. These concern the nature of phase transition between trivial and nontrivial phases [48], the effect of disorder on the surfaces and on phase transitions, and the precise implications of the bulk-boundary correspondence [31].

It would be highly desirable to find possible experimental realizations of such CTPs. In the field of quantum bosonic SPTs [8], experimental realizations are so far limited to $(1+1)$D [11]. Being free from the stringent requirement of quantum coherence, and based on simple microscopic ingredients, the classical counterparts introduced here may prove easier to realize. Indeed, similar classical systems, such as artificial spin-ice systems, have been successfully realized [49–51] using ferromagnetic wires as well as tiling molecules [52]. The 2D model we discussed could potentially be realized from the same microscopic ingredients.

Finally, it would be interesting to further explore the classification question we propose in this work, for instance, by considering other types of symmetries and constraints. Certainly there should be some relation with the group-cohomology classification of bosonic SPTs with a trivial bulk [8], however, it may not be one to one. Indeed, some SPTs may suffer from sign problems in Monte Carlo while others do not. Conversely, it may be that enforcing hard constraints or gauge symmetries allows for new types of quantum phases. Indeed, hard constraints in classical systems may result in a genus-dependent ergodicity breaking [53,54] whereas genus-dependent ground-state degeneracy is not part of the cohomology classification of Ref. [8].

ACKNOWLEDGMENTS

We are grateful to P. Fendley, T. Scaffidi, and S. H. Simon for stimulating discussions. Z.R. was supported by the European Union's Horizon 2020 research and innovation programme under the Marie Sklodowska-Curie grant Agreement No. 657111. R.B. was supported by the EPSRC Grants No. EP/I031014/1 and No. EP/N01930X/1.

Both authors contributed equally to this work.

APPENDIX: GENERAL DEFINITION OF A LOCAL CONSTRAINT, CONFINEMENT, AND DECONFINEMENT

Here, we address the issue of how one generally defines a lattice constraint as well as confined and deconfined phases. A local constraint on a lattice can be abstracted as follows: First, one requires a local mapping from the degrees of freedom to group elements in G'. For the sake of simplicity, we take G' Abelian. This mapping should be local such that the value g_x obtained at point x involves degrees of freedom near x. Furthermore, it must be neutral such the product of g_x over a closed manifold yields the identity. The constraint is then the requirement that $g_x = I$ (I being the identity) at all positions x. A defect f_x is a local violation of this rule in which $g_x = f_x \neq I$. In the familiar context of 3D lattice gauge theories on a cubic lattice, this mapping would be a mapping between boxes and magnetic charges within them. A local defect would

thus be a particular box where the magnetic charge is f instead of the identity.

Confined and deconfined phases are defined, as usual, by the free-energy cost ΔF_l of taking two static opposite defects (f, f^{-1}) apart. Confinement is defined by a free-energy cost which increases as a positive power of the distance (l) and a deconfined phase is defined by a saturating free-energy cost. Just like in the case of broken symmetries, these define two distinct phases of matter which can only be connected through a phase transition. The simplest way to show this is to remove the constraint and instead introduce Lagrange multipliers at every point where the constraint is imposed as

$$\delta_{f,1} = \frac{1}{|G'|} \sum_{\lambda} \chi_\lambda(f), \tag{A1}$$

where λ goes through $|G'|$ values labeling the irreducible one-dimensional representations of G' and $\chi_\lambda(f)$ is the character. If $G' = \mathbb{Z}_N$, we simply have $\chi_\lambda(f = a^k) = e^{2\pi i \lambda k/N}$, where a is the generator of $\mathbb{Z}_N$. By the neutrality condition, the resulting partition function obeys a global symmetry G' shifting all the $\{\lambda_x\}$ by the same amount. Finally, ΔF_l is given by

$$e^{-\Delta F_l} = \langle \chi_{\lambda_0}(f) \chi_{\lambda_l}(f^{-1}) \rangle, \tag{A2}$$

and the confined phase translates into the phase with exponentially decaying λ_x correlations (i.e., no spontaneous symmetry breaking) and the deconfined phase becomes the spontaneous broken-symmetry phase.

[1] M. Z. Hasan and C. L. Kane, Rev. Mod. Phys. **82**, 3045 (2010).
[2] R. Ilan, F. de Juan, and J. E. Moore, Phys. Rev. Lett. **115**, 096802 (2015).
[3] Z. Wu, F. M. Peeters, and K. Chang, Appl. Phys. Lett. **98**, 162101 (2011).
[4] C. Ojeda-Aristizabal, M. S. Fuhrer, N. P. Butch, J. Paglione, and I. Appelbaum, Appl. Phys. Lett. **101**, 023102 (2012).
[5] L. Fu and C. L. Kane, Phys. Rev. Lett. **100**, 096407 (2008).
[6] S. Ryu, A. P. Schnyder, A. Furusaki, and A. W. W. Ludwig, New J. Phys. **12**, 065010 (2010).
[7] X.-L. Qi, Phys. Rev. Lett. **107**, 126803 (2011).
[8] X. Chen, Z.-C. Gu, Z.-X. Liu, and X.-G. Wen, Phys. Rev. B **87**, 155114 (2013).
[9] X. Chen, Z.-C. Gu, and X.-G. Wen, Phys. Rev. B **84**, 235128 (2011).
[10] N. Schuch, D. Pérez-García, and I. Cirac, Phys. Rev. B **84**, 165139 (2011).
[11] W. J. L. Buyers, R. M. Morra, R. L. Armstrong, M. J. Hogan, P. Gerlach, and K. Hirakawa, Phys. Rev. Lett. **56**, 371 (1986).
[12] A. B. Khanikaev, S. Hossein Mousavi, W.-K. Tse, M. Kargarian, A. H. MacDonald, and G. Shvets, Nat. Mater. **12**, 233 (2013).
[13] C. L. Kane and T. C. Lubensky, Nat. Phys. **10**, 39 (2014).
[14] D. Z. Rocklin, Bryan Gin-ge Chen, M. Falk, V. Vitelli, and T. C. Lubensky, Phys. Rev. Lett. **116**, 135503 (2016).
[15] R. Süsstrunk and S. D. Huber, Science **349**, 47 (2015).
[16] S. A. Skirlo, L. Lu, Y. Igarashi, Q. Yan, J. Joannopoulos, and M. Soljačić, Phys. Rev. Lett. **115**, 253901 (2015).
[17] M. C. Rechtsman, J. M. Zeuner, Y. Plotnik, Y. Lumer, D. Podolsky, F. Dreisow, S. Nolte, M. Segev, and A. Szameit, Nature (London) **496**, 196 (2013).
[18] Y. E. Kraus, Y. Lahini, Z. Ringel, M. Verbin, and O. Zilberberg, Phys. Rev. Lett. **109**, 106402 (2012).
[19] J. Paulose, A. S. Meeussen, and V. Vitelli, Proc. Natl. Acad. Sci. USA **112**, 7639 (2015).
[20] B. G.-g. Chen, N. Upadhyaya, and V. Vitelli, Proc. Natl. Acad. Sci. USA **111**, 13004 (2014).
[21] M. Hafezi, E. A. Demler, M. D. Lukin, and J. M. Taylor, Nat. Phys. **7**, 907 (2011).
[22] I. Affleck, T. Kennedy, E. H. Lieb, and H. Tasaki, Commun. Math. Phys. **115**, 477 (1988).
[23] F. Pollmann, E. Berg, A. M. Turner, and M. Oshikawa, Phys. Rev. B **85**, 075125 (2012).
[24] S. D. Geraedts and O. I. Motrunich, Ann. Phys. **334**, 288 (2013).
[25] L. van Hove, Physica (Amsterdam) **16**, 137 (1950).
[26] C. Itzykson and J. Drouffe, *Statistical Field Theory: Volume 1, From Brownian Motion to Renormalization and Lattice Gauge Theory* (Cambridge University Press, Cambridge, 1991).
[27] R. Savit, Rev. Mod. Phys. **52**, 453 (1980).
[28] X. Chen, Y.-M. Lu, and A. Vishwanath, Nat. Commun. **5**, 3507 (2014).
[29] J. B. Kogut, Rev. Mod. Phys. **51**, 659 (1979).
[30] Z. Ringel and S. H. Simon, Phys. Rev. B **91**, 195117 (2015).
[31] T. Scaffidi and Z. Ringel, Phys. Rev. B **93**, 115105 (2016).
[32] E. Fradkin and S. H. Shenker, Phys. Rev. D **19**, 3682 (1979).
[33] R. Baxter, *Exactly Solved Models in Statistical Mechanics*, Dover Books on Physics (Dover, New York, 2007).
[34] B. Nienhuis, J. Stat. Phys. **34**, 731 (1984).
[35] Y.-M. Lu and A. Vishwanath, Phys. Rev. B **86**, 125119 (2012).
[36] D. V. Else and C. Nayak, Phys. Rev. B **90**, 235137 (2014).
[37] N. Reshetikhin, arXiv:1010.5031.
[38] J. D. Noh and D. Kim, Phys. Rev. E **53**, 3225 (1996).
[39] R. Balian, J. M. Drouffe, and C. Itzykson, Phys. Rev. D **11**, 2098 (1975).
[40] J. C. Wang, L. H. Santos, and X.-G. Wen, Phys. Rev. B **91**, 195134 (2015).
[41] A. Coste, T. Gannon, and P. Ruelle, Nucl. Phys. B **581**, 679 (2000).
[42] R. B. Laughlin, Phys. Rev. B **23**, 5632 (1981).
[43] M. Levin and Z.-C. Gu, Phys. Rev. B **86**, 115109 (2012).
[44] A. Hatcher, *Algebraic Topology* (Cambridge University Press, Cambridge, 2002).
[45] A. Kapustin, arXiv:1403.1467.
[46] C. Yung and M. Batchelor, Nucl. Phys. B **435**, 430 (1995).
[47] Y. Honda and T. Horiguchi, Phys. Rev. E **56**, 3920 (1997).
[48] Y.-Z. You, Z. Bi, D. Mao, and C. Xu, Phys. Rev. B **93**, 125101 (2016).

[49] R. F. Wang, C. Nisoli, R. S. Freitas, J. Li, W. McConville, B. J. Cooley, M. S. Lund, N. Samarth, C. Leighton, V. H. Crespi, and P. Schiffer, Nature (London) **439**, 303 (2006).
[50] Y. Qi, T. Brintlinger, and J. Cumings, Phys. Rev. B **77**, 094418 (2008).
[51] C. Nisoli, R. Moessner, and P. Schiffer, Rev. Mod. Phys. **85**, 1473 (2013).
[52] M. O. Blunt, J. C. Russell, M. d. C. Giménez-López, J. P. Garrahan, X. Lin, M. Schröder, N. R. Champness, and P. H. Beton, Science **322**, 1077 (2008).
[53] R. Moessner and S. L. Sondhi, Phys. Rev. Lett. **86**, 1881 (2001).
[54] M.-S. Vaezi, G. Ortiz, and Z. Nussinov, Phys. Rev. B **93**, 205112 (2016).